Frequency-dependent anisotropy, attenuation and dispersion of seismic waves in porous fractured rocks

Boris Gurevich, Miroslav Brajanovski, Luke J. Brown and Gracjan Lambert, Curtin University, Perth, Australia

Abstract

Fractures in a porous rock can be modelled as very thin and highly porous layers in a porous background. Elastic moduli of such a fractured medium can be obtained using the result of Norris (1993) for wave propagation in periodically layered poroelastic media. When this porous fractured system is dry, it is equivalent to a transversely isotropic dry elastic porous material with linear-slip interfaces. When saturated with a liquid this system exhibits significant attenuation and velocity dispersion due to wave-induced fluid flow between pores and fractures. The characteristic frequency of such attenuation and dispersion depends on the background permeability, fluid viscosity, as well as fracture density and spacing. The theoretical results are in good agreement with numerical simulations using the reflectivity algorithm generalized to poroelasticity.

For randomly distributed microfractures the frequency dependent anisotropy can be modelled using a combination of low frequency predictions based on anisotropic Gassmann equations and a frequency correction based on the dispersion relationship of Hudson et al. (1996). Comparison with laboratory experiments confirms that this combined model gives an accurate prediction of saturated elastic properties and angular dependencies of elastic wave velocities versus frequency.

Introduction

Naturally fractured reservoirs have attracted an increased interest of exploration and production geophysics in recent years. In many instances, natural fractures control the permeability of the reservoir, while porosity controls the overall capacity. The effect of fractures on elastic properties of fluid-saturated porous reservoirs differs from their effect in non-porous elastic media due to fluid flow between pores and fractures. Due to this wave-induced fluid flow, the properties of porous rocks with aligned fractures exhibit frequency dependent anisotropy.

We propose two alternative models for the frequency dependent properties of fractured porous rocks. In the first model, we model fractures as highly porous thin layers in a porous background. If we assume that the porous medium is permeated by a periodic sequence of such fractures (layers), we can derive the elastic properties of the system using the results of Norris (1993) and White et al. (1975), who give expressions for the frequency dependent effective moduli of a periodically layered poroelastic medium. To validate our theoretical model of attenuation and dispersion, we perform numerical experiments using a poroelastic extension of OASES reflectivity software.

In the second model fractures are modelled as voids of specific (disk-like) geometry. Here we combine the low-frequency results of the first model with a model of Hudson et al. (1996) for velocity dispersion.

Fractures as thin porous layers

We model a porous medium with aligned fractures as a periodically stratified system of alternating thick layers of a finite-porosity material of type *b* representing background, and thin layers of a high-porosity material of type *c* representing cracks or fractures. Background properties are: the porosity ϕ_b, permeability κ_b, dry (drained) bulk modulus K_b, shear modulus μ_b, and thickness h_b. Fracture (crack) properties are the porosity ϕ_c, permeability κ_c, dry bulk modulus K_c, shear modulus μ_c, and thickness $h_c \ll h_b$. The spatial period of the system is $h = h_b + h_c$, and the linear fractions of the materials *b* and *c* are $l_b = h_b/h$ and $l_c = h_c/h$. Both background and fractures are assumed to be made of the same isotropic grain material with bulk modulus K_g, shear modulus μ_g and density ρ_g, and saturated with the same fluid with bulk modulus K_f, density ρ_f, and dynamic viscosity η. The aim of this paper is to compute frequency dependent elastic wave velocities in such system of layers in the limits $l_c \to 0$, and $\phi_c \to 1$.

Elastic waves in such a periodically layered and porous medium can be described by Biot's (1962) equations of poroelasticity with spatially periodic and piecewise constant coefficients. Norris's (1993) result can be used to relate the overall elastic properties of the layered system to the properties of materials *b* and *c*. The properties of the fractured medium can then be established by taking the small thickness limit $l_c \to 0$. In this limit, the contribution of the fractures can only be significant if at the same time $K_c \to 0$, and hence $\phi_c \to 1$.

To relate different parameters of material *c* (fractures) to the commonly used fracture properties (such as fracture density), we first consider the dry fractured medium.

Dry fractured porous medium

When both materials *b* and *c* are dry ($K_f = 0$), they behave as isotropic elastic layers. In the long wavelength limit the system of horizontal layers perpendicular to

the x_3 axis is equivalent to a transversely isotropic elastic solid with a stiffness matrix $\mathbf{c}^{dry}$. Elements of this symmetric matrix are:

$$c_{33}^{dry}=\left\langle\frac{1}{L}\right\rangle^{-1},\quad c_{11}^{dry}=c_{22}^{dry}=c_{12}^{dry}+\langle 2\mu\rangle,\quad c_{44}^{dry}=c_{55}^{dry}=\left\langle\frac{1}{\mu}\right\rangle^{-1},$$

$$c_{13}^{dry}=c_{23}^{dry}=c_{33}^{dry}\left\langle\frac{\lambda}{L}\right\rangle,\ c_{12}^{dry}=\frac{\left(c_{13}^{dry}\right)^2}{c_{33}^{dry}}+\left\langle\frac{2\mu\lambda}{L}\right\rangle,\ c_{66}^{dry}=\langle\mu\rangle,\quad (1)$$

where $\lambda=K-2\mu/3,\quad L=\lambda+2\mu,$ and angle brackets indicate weighted average $\langle N\rangle=l_bN_b+l_cN_c$ of the enclosed property N. By inverting the stiffness matrix $\mathbf{c}^{dry}$ and taking the limit $l_c\to 0$, we can write the compliance matrix $\mathbf{s}^{dry}$ of the dry fractured porous medium in the form:

$$\mathbf{s}^{dry}=\mathbf{s}_b^{dry}+\mathbf{s}_c^{dry},\quad (2)$$

where $\mathbf{s}_b^{dry}$ is compliance matrix for the (isotropic) material *b* (background), and $\mathbf{s}_c^{dry}$ is excess compliance matrix given by the linear slip interface theory (Schoenberg and Douma, 1998):

$$Z_N=\lim_{l_c\to 0}\frac{l_c}{L_c}=s_{c33}^{dry},\qquad Z_T=\lim_{l_c\to 0}\frac{l_c}{\mu_c}=s_{c44}^{dry}=s_{c55}^{dry},\quad (3)$$

where Z_N and Z_T are called excess normal and tangential fracture compliances, respectively. Equations (3) mean that the fractures in the dry porous background are modeled as very thin and very soft porous layers, and imply that in the limit $l_c\to 0$ the porosity $\phi_c\to 1$. Using equations (3), we can relate the solutions of Biot's equations of poroelasticity for the fluid-saturated medium to the excess fracture compliances.

Fluid effect

Whereas the dry rock is elastic, the fluid saturated rock is bound to exhibit frequency dependent attenuation and velocity dispersion due to the wave induced fluid flow between pores and fractures. Norris (1993) showed that in the low-frequency regime of Biot's theory the compressional wave modulus c_{33}^{sat} of a periodically layered fluid-saturated porous medium can be written in the form:

$$\frac{1}{c_{33}^{sat}}=\frac{1}{C_\infty}+\frac{2}{i\omega h}(R_b-R_c)^2\left(z_b\cot\frac{d_b}{2}+z_c\cot\frac{d_c}{2}\right)^{-1},\quad (4)$$

where for $j=b,c$

$$\frac{1}{C_\infty}=\left\langle\frac{1}{C}\right\rangle=\frac{l_b}{C_b}+\frac{l_c}{C_c},\quad D_j=\frac{\kappa_j}{\eta}M_j\left(\frac{L_j}{C_j}\right),\quad (5)$$

$$z_j=\frac{\eta}{\kappa_j}\left(\frac{D_j}{\omega}\right)^{1/2}e^{-i\pi/4},\quad d_j=\left(\frac{\omega}{D_j}\right)^{1/2}hl_je^{i\pi/4},\quad R_j=\frac{\alpha_jM_j}{C_j}.$$

In these equations ω is frequency, C_j is the fluid-saturated *P*-wave modulus of the material j given by Gassmann's equations:

$$C_j=L_j+\alpha_j^2M_j,\quad M_j^{-1}=\frac{\alpha_j-\phi}{K_g}+\frac{\phi}{K_f},\quad (6)$$

and $\alpha_j=1-K_j/K_g$ denotes Biot's effective stress coefficient. Effective *P*-wave modulus of the fractured medium can be obtained by taking the limit $l_c\to 0$ in equation (4). In this limit, and taking into account equations (3), we observe that:

$$\kappa_c\gg\kappa_b,\quad M_c\to K_f,\quad D_c\to\frac{\kappa_c}{\eta}L_c,\quad |d_c|\ll 1,\quad R_c\to 1,$$

so that the modulus c_{33}^{sat} can be written in the form:

$$\frac{1}{c_{33}^{sat}}=\frac{1}{C_\infty}+\frac{\left(\frac{\alpha_bM_b}{C_b}-\frac{K_f}{C_c}\right)^2}{\frac{1}{Z_N}+\frac{L_bM_b}{C_b}\frac{h}{2J_b}\sqrt{i}\cot\left(\frac{h}{2J_b}\sqrt{i}\right)},\quad (7)$$

where the parameter J_b corresponds to the fluid diffusion length in the background material $J_b=\sqrt{\kappa_bM_bL_b/(\eta C_b\omega)}$. Further evaluation of the result expressed by equation (7) requires information about the saturating fluid. If the fractured porous continuum is dry, then $C_c\to L_c,$ and we have:

$$\frac{1}{c_{33}^{sat}}=\frac{1}{C_\infty}+Z_N=\frac{1}{L_b}+Z_N\quad (8)$$

in accordance with equation (3). On the other hand, if the fluid is liquid, so that in the limit $l_c\to 0$ its bulk modulus K_f is larger than that of the fracture material *c*, then $C_c\to K_f,\ C_\infty\to C_b,$ and we have:

$$\frac{1}{c_{33}^{sat}}=\frac{1}{C_b}+\frac{\left(\frac{\alpha_bM_b}{C_b}-1\right)^2}{\frac{1}{Z_N}+\frac{L_bM_b}{C_b}\frac{h}{2J_b}\sqrt{i}\cot\left(\frac{h}{2J_b}\sqrt{i}\right)}.\quad (9)$$

Here and below we will assume that K_f is finite. Equation (9) gives the *P*-wave modulus for waves propagating normal to fractures as a function of frequency, background properties and normal fracture compliance Z_N. The corresponding *P*-wave velocity along the symmetry axis x_3 is given by:

$$V_{p3}=\sqrt{\frac{C_{33}^{sat}}{\rho_b}},\quad (10)$$

where $\rho_b=\rho_g(1-\phi_b)+\rho_f\phi_b$ is mass density of the fluid-saturated background material. This velocity is complex and frequency dependent, indicating the presence of attenuation and dispersion.

Seismic frequencies

Of particular interest for seismic exploration are low-frequency elastic properties of porous fractured rocks. Elastic stiffness c_{33}^{sat} in the low frequency limit can be obtained from equation (9) by setting J_b to infinity. Similar results can be obtained for other elements of the stiffness matrix (Brajanovski and Gurevich, 2003). These results are consistent with the anisotropic Gassmann equations (Gassmann, 1951; Brown and Korringa, 1975; Gurevich, 2002). The most important conclusion from these results is strong influence of background porosity on the anisotropy of the fractured porous medium.

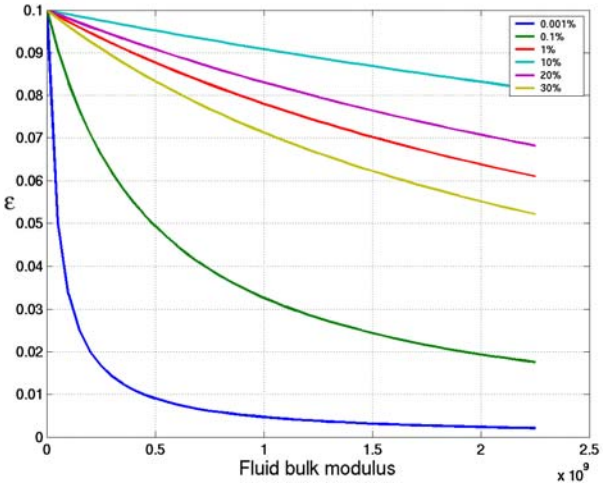

Figure 1. *P*-wave anisotropy parameter ε versus fluid bulk modulus for different values of the background porosity. For each porosity the fracture compliances have been adjusted to provide the same value of $\varepsilon = 0.1$ for the dry rock.

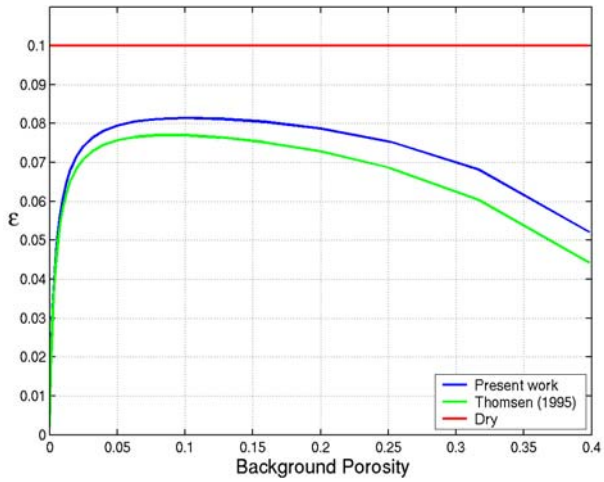

Figure 2. P-wave anisotropy parameter ε versus background porosity as predicted by the present theory (blue line), and Thomsen's (1995) theory (green line). Red line shows ε for the dry rock. For each porosity the fracture compliances have been adjusted to provide the same value $\varepsilon = 0.1$ for the dry rock.

Figure 1 shows *P*-wave anisotropy parameter ε of the porous fractured medium saturated with a fluid of bulk modulus K_f for different background porosities. For each porosity a different value of normal fracture compliance was used to produce the same value for $\varepsilon^0 = 0.1$ for the dry medium and fracture porosity of 0.01 % (this corresponds to crack density of penny-shaped cracks equal to 0.0375). At very low background porosities, ε^{sat} tends to zero as K_f increases. However, even for modest values of background porosity ε^{sat} shows a much more gradual decrease with increasing fluid modulus. Interestingly, the decrease of ε^{sat} with K_f is minimal at around 10 % porosity, and then increases again.

Figure 2 examines this effect further. It presents ε as a function of background porosity ϕ_b for water-saturated rock ($K_f = 2.25 \times 10^9$ Pa). Blue line shows the solution based on anisotropic Gassmann equations (Gurevich 2002), and green line the solution of Thomsen (1995). We see that ε is zero for zero background porosity, and within a range of a few per cent porosity sharply increases to almost ε^0, the value of ε for the dry medium. Then the dependency of ε on ϕ_b levels off and before gradually decreasing to about half of ε^0 at background porosity about 40%.

As discussed by Thomsen (1995) and Hudson et al. (2001), the sharp increase of ε results from the fact that when surrounded by (equant) pores, the fluid in the fracture has plenty of space around it to escape to when compressed, and therefore the fracture is almost as compliant as in the dry medium. In other words, stiffening of compliant pores by the fluid does not occur, as fluid can escape into the pores. This effect is most pronounced between zero and 5-10% porosity.

The gradual decrease of ε at higher background porosities is simply the result of fluid saturation: the more porous the rock, the greater the role of the saturating fluid in the overall properties of the rock. Since the pore fluid is isotropic, it tends to reduce the overall degree of anisotropy of the rock.

Velocity dispersion and attenuation

For the *P*-wave modulus along the symmetry axis frequency dependence is given by equation (9), which can also be written in the form

$$\frac{1}{c_{33}^{sat}} = \frac{1}{C_b} + \frac{\Delta_N \left(\frac{\alpha_b M_b}{C_b} - 1\right)^2}{L_b \left[1 - \Delta_N + \Delta_N \sqrt{i\omega'} \cot\left(\frac{C_b}{M_b}\sqrt{i\omega'}\right)\right]}. \qquad (11)$$

Here we have introduced a dimensionless fracture weakness Δ_N and the normalized frequency ω':

$$\Delta_N = \frac{L_b Z_N}{1 + L_b Z_N}, \qquad \omega' = \frac{h^2 \eta M_b \omega}{4\kappa_b C_b L_b}. \qquad (12)$$

Equation (11) can be used to evaluate the frequency dependence of the *P*-wave velocity and attenuation for

waves propagating perpendicular to fractures from the equations:

$$V_p = \left(\mathrm{Re}\left(V_{p3}^{-1}\right)\right)^{-1}, \quad Q^{-1} = 2V_p \mathrm{Im}\left(V_{p3}^{-1}\right), \tag{13}$$

where V_{p3} is complex velocity given by equation (10). Figures 3(a, b) show velocity normalised by the high-frequency velocity $V_p^{\infty} = \left(c_{33}^{\infty}/\rho\right)^{1/2}$ and dimensionless attenuation Q^{-1} as functions of normalised frequency, for a water-saturated quartz sandstone ($K_g = 37$ GPa, $\mu_g = 44$ GPa, $\rho_g = 2.65$ g cm^{-3}). with dry fracture weakness $\Delta_N = 0.2$ and different background porosity levels. The dependency of the background dry bulk and shear moduli on porosity was assumed to follow the empirical model of Krief et al. (1990) $K_b/K_g = \mu_b/\mu_g = (1-\phi)^{3/(1-\phi)}$. Velocity dispersion and attenuation have a shape typical for a relaxation phenomenon.

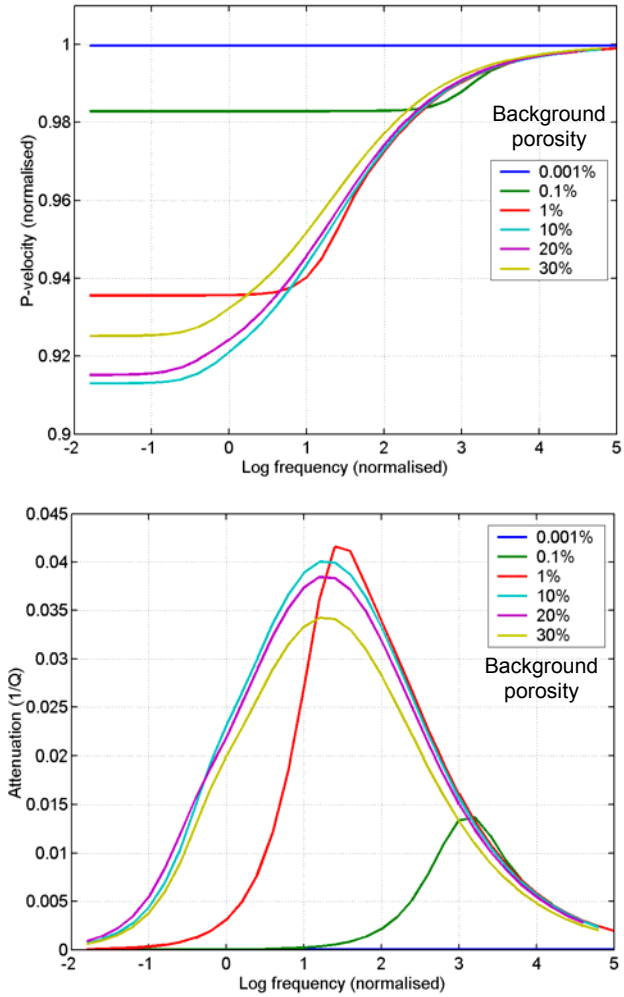

Figure 3: (a) P-wave velocity dispersion for fixed fracture weakness and varying background porosity (b) attenuation for the same medium

For the constant Δ_N, both attenuation and dispersion increase sharply with increasing porosity from zero up to a few per cent porosity, and have almost identical shapes for porosities higher than 10%. The calculations were made We also note that the dispersion and attenuation are significant over a frequency range that spans at least two orders of magnitude. The results for various levels of Δ_N are shown in more detail in Figures 4 (a, b) for typical reservoir background porosity of 20%. As expected, the dispersion and attenuation are proportional to the fracture weakness Δ_N The peak normalised frequency for attenuation decreases with increasing fracture weakness.

Numerical simulations

To validate our asymptotic theoretical model of attenuation and dispersion, we perform numerical experiments using a poroelastic extension (Stern et al., 1985) of OASES reflectivity software (Schmidt and Tango, 1986), which can compute the plane-wave transmission coefficient for a stack of porous layers with given thicknesses.

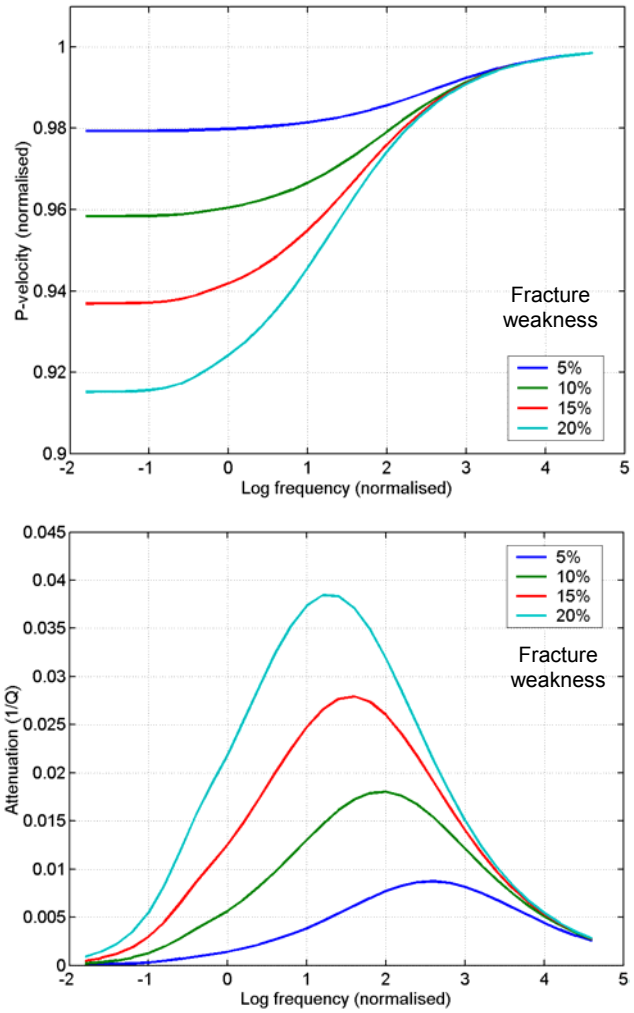

Figure 4: (a) P-wave velocity dispersion for fixed porosity and varying fracture weakness (b) attenuation for the same medium.

We simulate a seismic wave propagating normally to the periodic stack of 48 alternating porous fluid-saturated layers, of which 24 thick layers represent background (with porosity 20%) and 24 thin highly porous equidistant layers represent fractures with normal fractures weakness 0.1. Figure 5 compares effective attenuation $1/Q$ calculated from the transmission coefficient computed by OASES with our theoretical prediction based on equation (11). We observe good agreement between our effective medium theory for fractured rock and the numerical experiment. Moreover, similar results were obtained for randomly as well as periodically distributed fractures. This means that the results obtained for periodic systems of fractures apply to much more general fracture systems.

Fractures as penny-shaped cracks

Hudson et al. (1996) developed a theory for frequency dependent elastic properties of porous rocks with penny-shaped cracks. This theory is based on analysis of the fluid pressure relaxation between a single crack and the unbounded porous continuum (background). As a result of this analysis, Hudson et al. (1996) obtained anisotropy parameters of the fractured medium as functions of frequency. In the low frequency limit, the model predicts equal anisotropy in the dry and saturated media, a result which is inconsistent with the anisotropic Gassmann equations (Hudson et al., 2001).

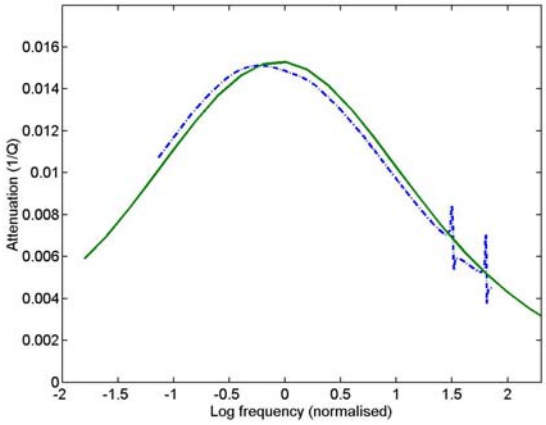

Figure 5: Attenuation computed using reflectivity method (blue line) and predicted by the effective medium theory (green line).

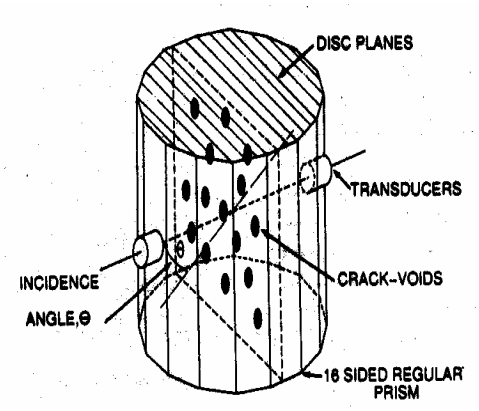

Figure 6. Experimental setup for ultrasonic measurements of Rathore et al. (1995)

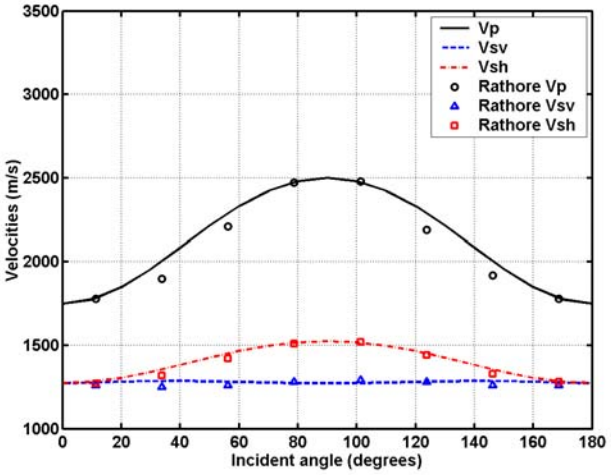

Figure 7. P, SH, and SV velocities versus angle for dry sample. Symbols: measured data, lines: linear slip fit.

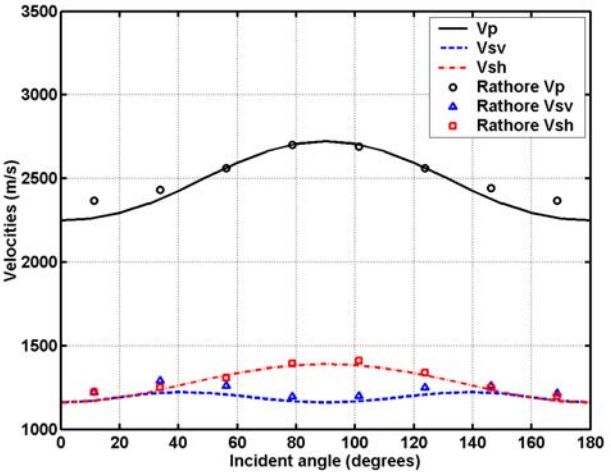

Figure 8. P, SH, and SV velocities versus angle for water-saturated sample. Symbols: measured data, lines: anisotropic Gassmann prediction.

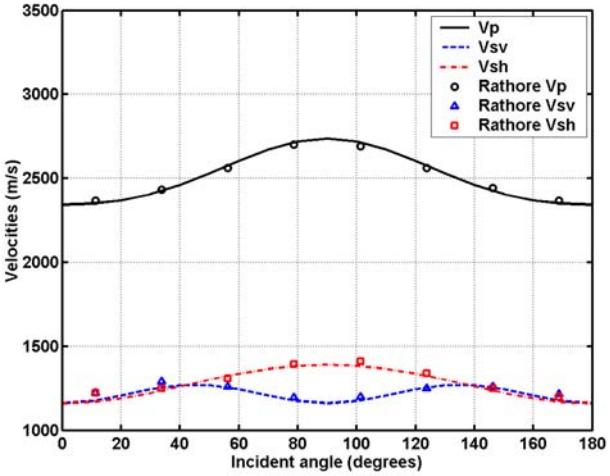

Figure 9. P, SH, and SV velocities versus angle for water-saturated sample. Symbols: measured data, lines: anisotropic Gassmann prediction with frequency correction

This discrepancy arises from the single crack analysis which is only applicable when wavelength is small compared to the distance between cracks (Hudson et al., 2001). However, the relative velocity dispersion (frequency dependency) predicted by Hudson et al. (1996) is realistic. In order to model the frequency dependent anisotropy in a manner consistent with the anisotropic Gassmann equations, we combine the dispersion relationship of Hudson et al. (1996) with the low-frequency results of the present study.

We test this combined model on the experimental data of Rathore et al. (1995). The experiment measured compressional and shear wave velocities as functions of angle on a dry and saturated synthetic porous rock sample with aligned but randomly distributed disc shaped cracks (Figure 6). The ultrasonic data were recorded using a central frequency of 100 kHz. The physical properties of the uncracked background and fractures were measured in the experiment, and dry fracture weaknesses were obtained from the best fit of dry velocities as functions of angle (Figure 7). The elastic properties of the saturated sample were then predicted using the derivations of the present study. Figure 8 shows the prediction of saturated compressional and shear wave velocities based low-frequency anisotropic Gassmann equations (Gurevich, 2002). There is a reasonably good fit for the orthogonally polarised shear waves, but anisotropy of the compressional wave is overestimated. Figure 9 again shows velocities obtained from saturated elastic properties, but after the frequency correction based on the results of Hudson et al. (1996). Excellent agreement is observed. Note that unlike the study of Hudson et al. (2001), who used permeability values that provided best fit with measured velocities, our prediction is based on the measured matrix permeability of 11.4 Darcy.

Conclusions

Fractures in porous rocks can be modelled as very thin and highly porous layers in a porous background. Such a medium saturated with a liquid exhibits significant attenuation and velocity dispersion due to wave induced fluid flow between pores and fractures. At low frequencies the elastic properties are equal to those obtained by anisotropic Gassmann theory applied to a porous material with linear-slip interfaces. At high frequencies the results are equivalent to those for fractures in a solid (non-porous) background. The characteristic frequency of the attenuation and dispersion depends on the background permeability, fluid viscosity, as well as fracture density and spacing. The theoretical results are in good agreement with numerical simulations based on the reflectivity method generalized to poroelasticity. Moreover these experiments confirm that the results are valid for both periodic and random fracture systems.

For randomly distributed penny-shaped cracks the frequency-dependent anisotropy can be modelled using a combination of low-frequency anisotropic Gassmann theory and a frequency correction based on the dispersion relationship of Hudson et al. (1996). Predictions of this combined model are in an excellent agreement with ultrasonic experimental results of Rathore et al. (1995).

Acknowledgments

Financial support of the Centre for Mining Technology and Equipment, CSIRO Petroleum, Centre of Excellence for Exploration and Production Geophysics, and Australian Petroleum Cooperative Research Centre is gratefully acknowledged. The authors thank Michael Schoenberg and Erling Fjær for useful advice.

References

Biot, M. A., 1962, Mechanics of deformation and acoustic propagation in porous media: J. Appl. Phys., 33, 1482-1498.

Brown, R. J. S. and Korringa, J., 1975, On the dependence of the elastic properties of a porous rock on the compressibility of the pore fluid: Geophysics, 40, 608-616.

Brajanovski, M., and Gurevich, B., 2003, Frequency dependent anisotropy of porous rocks with aligned fractures, Submitted to Exploration Geophysics.

Gassmann, F., 1951, Über die Elastizität poröser Medien: Viertel. Naturforsch. Ges. Zürich, 96, 1-23.

Gurevich, B., 2002, Elastic properties of saturated porous rocks with aligned fractures: 72d Ann. Mtg., Soc. Eexpl. Geophys., Expanded Abstracts, Paper ANI P1.6.

Hudson, J.A., Liu, E., and Crampin, S., 1996, The mechanical properties of materials with interconnected cracks and pores: Geophys. J. Internat., 124, 105-112.

Hudson, J.A., Pointer, T., and Liu, E., 2001, Effective medium theories for fluid saturated material with aligned cracks: Geophys. Prosp., 49, 509-522.

Krief, M., Garat, J., Stellingwerff, J. and Venture, J., 1990, A petrophysical interpretation using the velocities of P and S waves (full waveform sonic): The Log Analyst, 31, 355-369.

Norris, A. N., 1993, Low frequency dispersion and attenuation in partially saturated rocks: J. Acoust. Soc. Amer., 94, 359-370.

Rathore, J.S., Fjær, E., Holt, R.M., and Renlie, L., 1995, P- and S-wave anisotropy of a synthetic sandstone with controlled crack geometry: Geophys. Prosp., 43, 711-728.

Schmidt, H. and Tango, G., 1986, Efficient global matrix approach to the computation of synthetic seismograms: Geophys. J. Roy. Astr. Soc., 84, 331-359

Schoenberg, M. and Douma, J., 1988, Elastic wave propagation in media with parallel fractures and aligned cracks: Geophys. Prosp., 36, 571-590.

Stern, M., Bedford, A. and Millwater, H.R., 1985, Wave reflection from a sediment layer withdepth-dependent properties: J. Acoust. Soc. Amer., 77, 1781–1788.

Thomsen, L., 1995, Elastic anisotropy due to aligned cracks in porous rock: Geophys. Prosp., 43, 805-829.

White, J. E., Mikhaylova, N. G. and Lyakhovitsky, F.M., 1975, Low-frequency seismic waves in fluid-saturated layered rocks: Izvestija Academy of Sciences USSR, Phys. Solid Earth, 11 (10), 654-659.